



## Research article

# Identification of key biomarkers of endothelial dysfunction in hypertension with carotid atherosclerosis based on WGCNA and the LASSO algorithm

Yimin Wang<sup>a,1</sup>, Xinyang Shou<sup>b,1</sup>, Yuteng Wu<sup>b</sup>, Jun Chen<sup>b</sup>, Rui Zeng<sup>a</sup>, Qiang Liu<sup>a,\*</sup><sup>a</sup> The Third Affiliated Hospital of Zhejiang Chinese Medical University, Hangzhou, Zhejiang, 310005, China<sup>b</sup> Zhejiang Chinese Medical University, Hangzhou, Zhejiang, 310053, China

## ARTICLE INFO

## Keywords:

Endothelial dysfunction  
Carotid atherosclerosis  
Hypertension  
Bioinformatics  
Hub genes

## ABSTRACT

**Background:** Endothelial dysfunction is the early stage of carotid atherosclerosis (CAS) in patients with hypertension. It is worth identifying the potential hub genes of endothelial dysfunction to elucidate pathological mechanism in the progression of the disease.

**Method:** We obtained gene expression profiles of GSE43292 from the Gene Expression Omnibus (GEO) database. Hub genes associated with CAS were identified through weighted gene correlation network analysis (WGCNA) and least absolute shrinkage and selection operator (LASSO) regression. Subsequently, Gene Ontology (GO) and Kyoto Encyclopedia of Genes and Genomes (KEGG) enrichment analyses were performed to explore potential biological mechanisms and signaling pathways. Finally, *in vitro* experiments on human umbilical vein endothelial cells (HUVECs) were conducted to validate these hub genes.

**Results:** The microarray dataset GSE43292 included 32 CAS plaques samples and corresponding macroscopically intact tissues from patients with hypertension. A total of 161 differentially expressed genes were discovered. Through WGCNA analysis, the gray60 module emerged as the most significant module associated with clinical features. The GO and KEGG enrichment analyses of genes in the gray60 module highlighted the substantial involvement of immune response-related signaling pathways. Two key hub genes (CCR1 and NCKAP1L) were pinpointed *via* LASSO regression. We found a significant increase in the mRNA expression level of the hub genes in oxidized low density lipoprotein (ox-LDL) treated HUVECs.

**Conclusions:** Our study indicated that the hub genes related to immune responses are involved in the development of CAS. Two hub genes (CCR1 and NCKAP1L) of endothelial dysfunction were identified. These genes may provide a valuable therapeutic target of CAS in patients with hypertension.

## 1. Introduction

Both hypertension and carotid atherosclerosis (CAS) are major risk factors for ischemic stroke, contributing to large part of stroke cases [1,2]. A previous study has shown that hypertension is also a risk factor for CAS [3]. Elevation of vascular laminar shear stress

\* Corresponding author. No. 297 Moganshan Road, Hangzhou, Zhejiang, 310005, China.

E-mail address: [19981011@zcmu.edu.cn](mailto:19981011@zcmu.edu.cn) (Q. Liu).

<sup>1</sup> These authors contributed equally to this work and share first authorship.

caused by hypertension leads to an increase in oxidative stress and the occurrence of endothelial dysfunction [4,5]. Atherosclerosis can impair the stretch of the baroreceptors, leading to reduced neural input to the autonomic control centers in the brain stem. The reduction in autonomic output to the cardiovascular system results in more pronounced blood pressure fluctuations [6]. Vascular endothelial cells become activated in response to injurious stimuli or local hemodynamic alterations. Consequently, chemokines are released to specifically attract circulating monocytes from the bloodstream to the intima, where they progressively transform into foam cells, initiating the formation of early atherosclerotic lesions on a macroscopic scale [7]. In the advanced stages of the lesion, endothelial cell apoptosis disrupts the integrity of the endothelial monolayer, prompting endothelial denudation and the development of atherothrombotic occlusions. Therefore, identifying the molecular biomarkers of endothelial dysfunction is of paramount importance [8,9].

With the continuous application of gene technology in bioinformatics, new biomarkers of common diseases have been precisely screened and can be used as an important target spot for clinical diagnosis or treatment [10]. In this study, we downloaded the microarray data from the Gene Expression Omnibus (GEO) database, and preliminarily determined genes related to hypertension with CAS through difference analysis and weighted correlation network analysis (WGCNA). Gene Ontology (GO) and Kyoto Encyclopedia of Genes and Genomes (KEGG) pathway analyses on the genes of key modules in the coexpression network were carried out to explore the potential biological functions of these genes. After that, a protein–protein interaction network was created, and hub genes were mined using Molecular Complex Detection (MCODE). The least absolute shrinkage and selection operator (LASSO) regression analysis was also conducted to analyze the correlation between the hub genes and clinical characteristics. Finally, an atherosclerotic endothelial dysfunction model was established, and quantitative real-time polymerase chain reaction (qRT-PCR) validation was used to evaluate the selected biomarkers. In conclusion, our study identified novel biomarkers associated with the immune response in endothelial dysfunction, presenting promising potential as effective therapeutic indicators for hypertension with CAS.

## 2. Material and methods

### 2.1. Data source

The thorough study design is illustrated in Fig. 1. The gene expression profile dataset, GSE43292, was sourced from the GEO database (<https://www.ncbi.nlm.nih.gov/geo>). The GSE43292 dataset included 32 carotid atheromatous plaques (stage IV and over of the Stary classification) and corresponding macroscopically intact tissues from patients with hypertension. The samples belonged to a heterogeneous population of cells contained in the media and neo-intima without adventitia.

### 2.2. Screening of differentially expressed genes (DEGs)

First, raw data of GSE43292 were processed utilizing the robust multi-array average (RMA) expression measure function in the

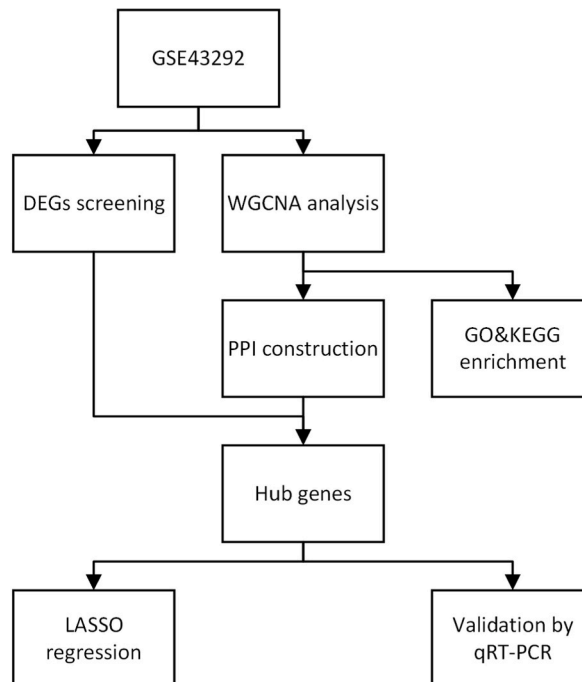


Fig. 1. The flowchart of the entire study.

“affy” R package [11]. After removing the batch effects with the “sva” R package, a principal component analysis (PCA) plot was created. Finally, the “limma” R package was utilized to investigate DEGs between atheroma plaques and corresponding macroscopically intact tissues under the threshold of “ $|\log_2(\text{fold change})| > 1$  and  $P < 0.05$ ” [12]. Volcano plot and heat map were depicted to show the significant genes. All analyses of data were processed in R (v4.1.3).

### 2.3. Coexpression network construction by WGCNA

The genes with the top 5000 variance were filtered and clustered to identify the coexpression network using the “WGCNA” package [13]. After the scale-free network was established, a cluster tree dendrogram was built with the minimal gene module size of 30 and the threshold of 0.25. The module membership (MM) and gene significance (GS) were calculated to evaluate the relevance between the key modules and clinical features.

### 2.4. Functional and pathway enrichment analysis

GO and KEGG analyses were employed using “cluster Profiler” and “GO plot” package for genes in the gray60 module [14]. The top 20 significant terms with the  $p$ -value cutoff  $< 0.05$  and count  $\geq 10$  were determined. The difference in coexpression patterns between atheroma plaques and their corresponding macroscopically intact tissues from patients with hypertension were analyzed based on these results.

### 2.5. Construction of protein–protein interactions network and screening of hub genes

The STRING database version 11.5 (<https://version-11-5.string-db.org/>) was used to construct the protein–protein interactions (PPI) network with the medium confidence (interaction  $> 0.4$ ) of sig genes [15]. Then, the PPI network was downloaded from STRING and visualized using Cytoscape version 3.10.0 [16]. The MCODE algorithm, a plugin in Cytoscape to detect densely connected sub-network, was used to identify the MCODE genes [17], which were intersected with DEGs to obtain the hub genes.

### 2.6. LASSO regression analysis

LASSO algorithm was performed to streamline the clinical characteristic variables to identify the hub genes by R package “glmnet” [18]. The optimal lambda was calculated with a minimum value of 10-fold cross-validation in the training set. The GSE43292 dataset was randomly split into training and validation groups at a proportion of 1:1.

### 2.7. Cell culture and transwell experiments

Human umbilical vein endothelial cells (HUVECs) were obtained from the Cell Resource Center, Peking Union Medical College (PCRC) on October 13th, 2022. Based on previous research methods [19], HUVECs were cultured in high-glucose DMEM (C11995500BT, Gibco, Shanghai, China) supplemented with 10 % FBS (11011-8611, Tianhang, Zhejiang, China) at 37 °C in 5 % CO<sub>2</sub>. HUVECs were seeded in chambers (#14321, Labselect, Anhui, China) and grown with 100 µg/mL low density lipoprotein (ox-LDL) (YB-002, Yiyuan Biotech. Co. Ltd, Guangdong, China) for 24 h. HUVECs were incubated with 4 % paraformaldehyde at 23 °C for 15 min. Then, the chamber was immersed in PUS for washing three times. Subsequently, HUVECs were permeated with anhydrous methanol at 23 °C for 20 min. Next, 0.5 % crystal violet was added to stain the bottom of the chamber for 10 min, and the chamber was thoroughly washed three times with PBS. Images were obtained under a microscope (Olympus, Tokyo, Japan) and analyzed using ImageJ software, version 1.53t (NIH, Bethesda, MD, USA).

### 2.8. Quantitative real-time PCR

Total RNA was extracted using Trizol (R0016, Beyotime Biotechnology, Shanghai, China) in accordance with the manufacturer’s instructions and precipitated with isopropanol. After converting RNA into cDNA using the Evo M-MLV RT Premix kit (AG11706, Accurate Biotechnology, Hunan, China), qRT-PCR analysis was performed using the SYBR Green Premix Pro Taq HS qPCR Kit (AG11701, Accurate Biotechnology) in the Roche LightCycler 96 system (Roche, Basel, Switzerland). Table 1 lists all primer sequences used in this study, *CCR1* and *NCKAP1L* (Sangon Biotech, Shanghai, China). The relative expression of each gene was evaluated by comparing its expression with that of *ACTB* using the  $2^{-\Delta\Delta Ct}$  method.

**Table 1**  
Primer sequences.

Primer	Forward (5′–3′)	Reverse (5′–3′)
CCR1	ATCCTGTTGACGATTGACAGAT	TGATGCCAAAAGTAACAGTTTCG
NCKAP1L	CGTGGAAAGTGATGGAGCGATGG	CTTCTGGCACTGGCTGTTGGAG

2.9. Statistical analysis

All data are represented as mean ± SEM unless otherwise noted. Independent-sample *t*-test and analysis of variance were used to establish statistical significance. The GraphPad Prism software version 8.0.2 was used to perform all statistical analyses (GraphPad, San Diego, CA, USA). All experiments were conducted independently in triplicate.

3. Results

3.1. Identification of DEGs

The profiles of GSE43292 were processed and standardized (Fig. 2A). As demonstrated in the volcano plots, 161 DEGs were eventually identified in GSE43292 under the threshold of “|log<sub>2</sub>(fold change)| > 1 and *p* < 0.05,” including 82 upregulated genes and 79 downregulated genes (Fig. 2B). Heat map of the top 50 DEGs by *p* value are displayed in Fig. 2C. PCA revealed distinct segregation into two groups between carotid atheromatous plaques and macroscopically intact tissues of patients with hypertension (Fig. 2D).

3.2. Identification of CAS-related gene modules

Two outliers, GSM1060123 and GSM1060169, were detected (Fig. 3A). Then, the soft-threshold power β = 16 and cutoff R<sup>2</sup> = 0.8 were selected to reach the requirements of scale-free topology (Fig. 3B). Eleven modules were identified by creating TOM matrices and merging similar dynamic dendrogram tree (Fig. 3C). Then, the correlation between each module and clinical traits was evaluated by Pearson’s correlation analysis. As shown in Fig. 3D, the gray60 module exhibited strong positive connection with CAS in patients with

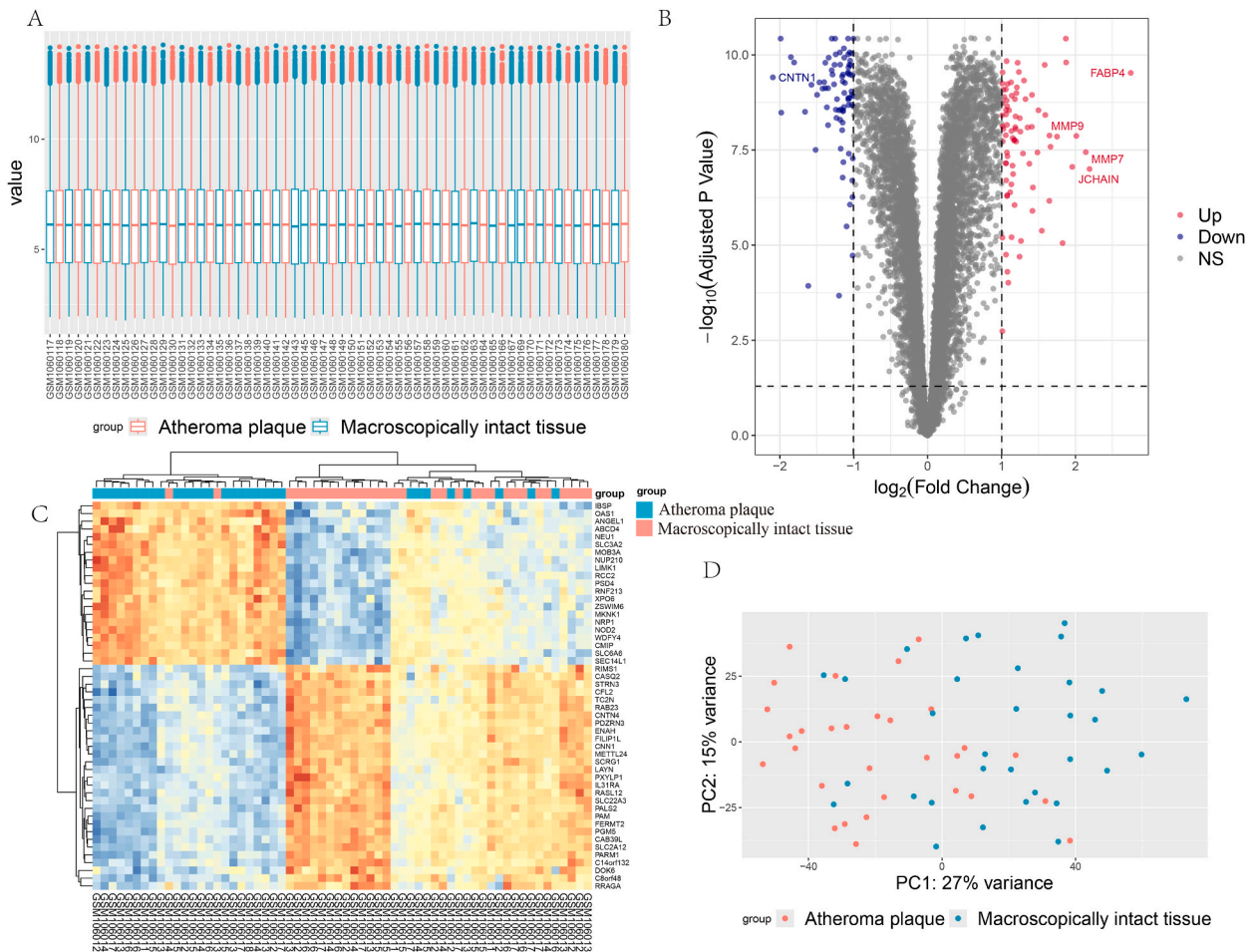


**Fig. 2.** Identification of DEGs. (A) Box plot of GSE43292 gene expression data after standardization. Red bars represent CAS plaques samples, and blue bars represent their corresponding macroscopically intact tissues. (B) Volcano plot of DEGs in CAS plaques from patients with hypertension compared with controls. (C) Heat map of top 50 DEGs (upregulated and downregulated). (D) PCA plot of gene expression data.

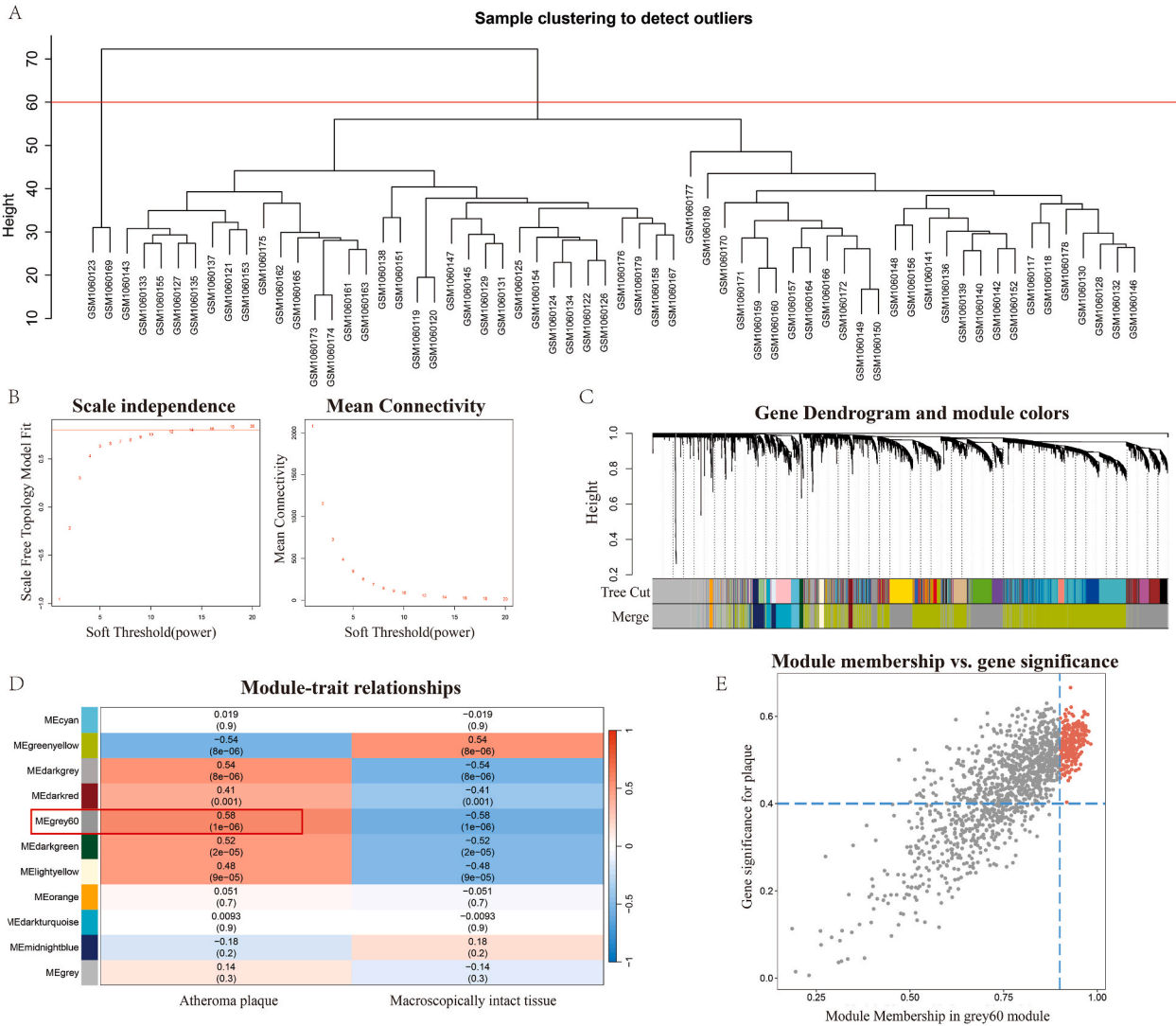


**Fig. 3.** Construction of the coexpression network for GSE43292. (A) Two outliers (GSM1060123 and GSM1060169) were detected using clustering, and other samples were included in the further study. (B) Soft-thresholding power for scale-free topology was 16, and the best cutoff R2 was 0.8. (C) Eleven gene modules were detected in GSE43292. (D) Significance values of the relationships between the 11 modules and CAS in the patients with hypertension. (E) Scatter plot between MM and GS in the gray60 module.

hypertension ( $P = 1e-06$ ). Next, 249 out of 1366 genes were filtered as  $|GS| > 0.4$  and  $|MM| > 0.9$  in the gray60 module, which were identified as significant genes. Fig. 3E shows the correlation between CAS in the patients with hypertension and the genes in the gray60 module ( $cor = 0.8, P < 1e-200$ ).

### 3.3. Functional enrichment of the gene modules

We found that 249 sig genes were mainly enriched in immune response–regulating signaling pathway, phagocytosis, myeloid cell activation involved in immune response, and immune response–activating signaling pathway. Subsequently, the pathway analysis showed that lysosome, B-cell receptor signaling pathway, chemokine signaling pathway, Fc epsilon RI signaling pathway, and platelet activation were enriched in the KEGG terms. The GO and KEGG pathway analyses with top 10 sig genes by  $P$  value are shown in Fig. 4A and B, and Table 2. There was a significant overlap of genes between signaling pathways of immune response (Fig. 4C), suggesting that the immune response signaling pathway may be involved in CAS in patients with hypertension. Moreover, the analyses showed that sig genes with high significance and network centrality correlated with immune response and phagocytosis, revealing the potential association of both pathways with the pathogenesis of CAS in patients with hypertension.

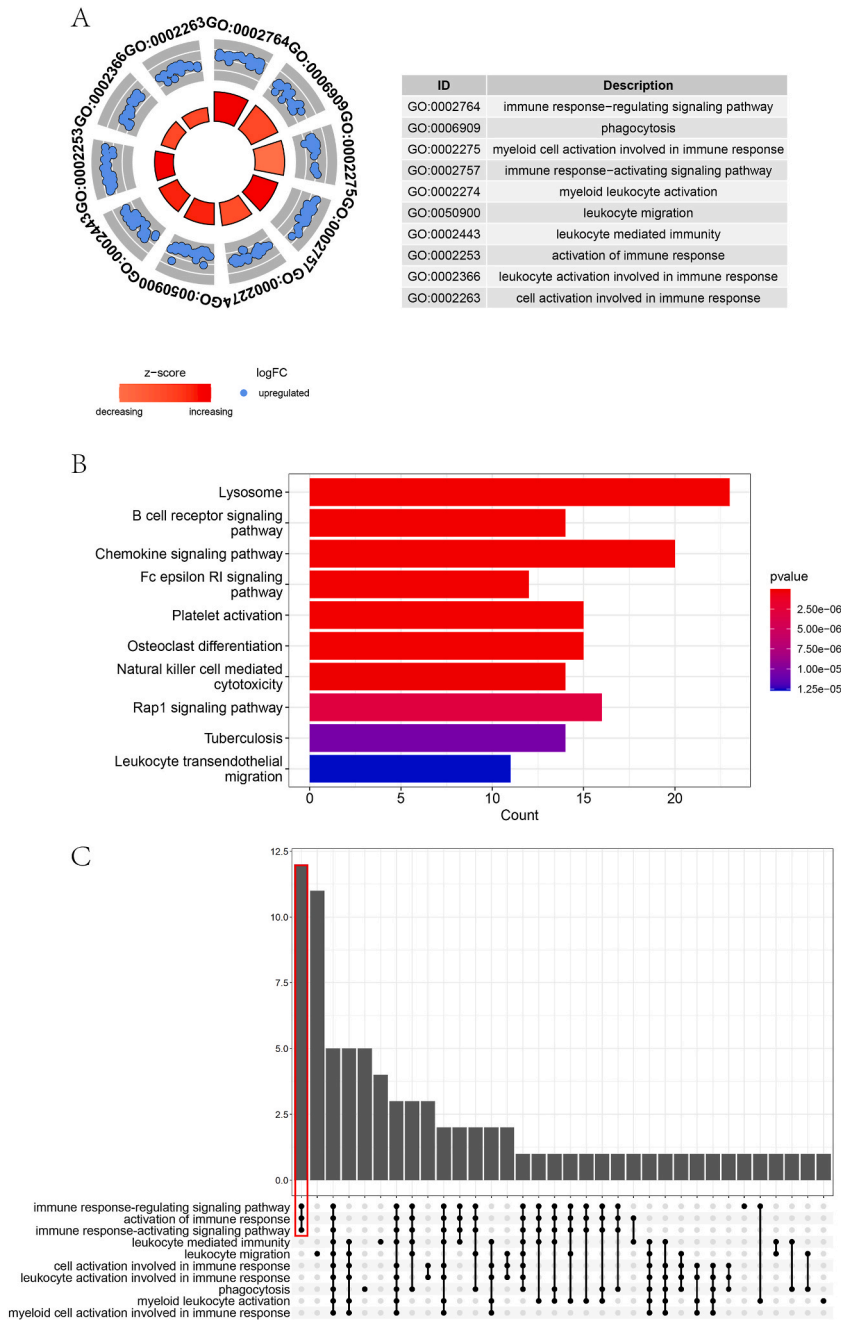


**Fig. 4.** Functional enrichment analysis of sig genes in the gray60 module. (A) GO bubble plot of GO analysis. (B) Bar plot of KEGG pathway analysis. (C) UpSet plot for GO functional annotation.

### 3.4. Construction of the PPI network and screening of hub genes

The sig genes' PPI network with 248 nodes and 1656 edges was generated by STRING (Fig. 5A). Subsequently, genes interaction data were downloaded and uploaded to Cytoscape, where 29 MCODE genes with the highest scores in interconnected cluster network were identified using the MCODE plugin (Fig. 5B). They were overlapped with the DEGs to obtain a total of six hub genes (NCKAP1L, ITGB2, CCR1, ITGAX, ITGAM, PLEK) (Fig. 5C-Table 3).

**Table 2**

GO and KEGG pathway analyses with top 10 sig genes by *P* value for the gray60 module of CAS in patients with hypertension.

Terms	<i>P</i> value	Count
<b>GO</b>		
immune response–regulating signaling pathway	4.89E-17	38
phagocytosis	4.89E-17	29
myeloid cell activation involved in immune response	4.89E-17	21
immune response–activating signaling pathway	1.53E-16	36
myeloid leukocyte activation	4.21E-16	28
leukocyte migration	6.76E-16	34
leukocyte-mediated immunity	1.09E-15	34
activation of immune response	1.76E-15	37
leukocyte activation involved in immune response	6.58E-15	29
cell activation involved in immune response	8.52E-15	29
<b>KEGG</b>		
lysosome	5.72E-14	23
B-cell receptor signaling pathway	3.45E-08	14
chemokine signaling pathway	3.45E-08	20
Fc epsilon RI signaling pathway	2.39E-07	12
platelet activation	4.66E-07	15
osteoclast differentiation	1.25E-06	15
natural killer cell–mediated cytotoxicity	5.70E-06	14
Rap1 signaling pathway	6.00E-05	16
tuberculosis	0.00019	14
leukocyte transendothelial migration	0.000244	11

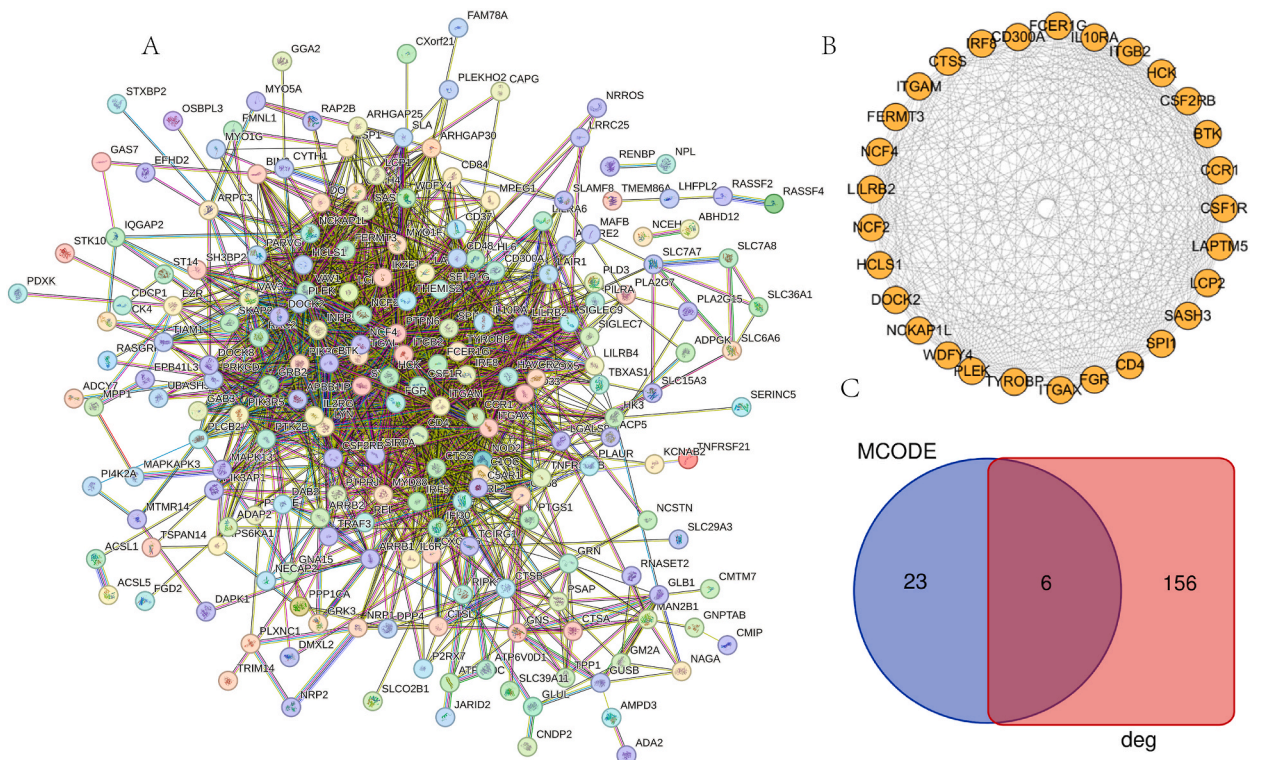


**Fig. 5.** Identification of six hub genes: (A) The PPI network of 249 genes screened from the gray60 module was obtained from the STRING database; (B) 29 genes were identified by MCODE; (C) intersection of MCODE genes and DEGs.

**3.5. Identification of CCR1 and NCKAP1L**

To further identify potential prognostic markers in the progression of CAS in patients with hypertension, the six hub genes were input into the LASSO regression analysis based on lambda.1se (0.1704954). Two hub genes were identified (CCR1, NCKAP1L) as the most representative of the genes involved in CAS in patients with hypertension (Fig. 6A and B). Box plots showed the expression levels

**Table 3**  
The summary of six hub genes.

Gene symbol	Official full name	logFC	P value
NCKAP1L	NCK-associated protein 1 like	1.06	8.05e-10
ITGB2	integrin subunit beta 2	1.06	2.80e-09
CCR1	C-C motif chemokine receptor 1	1.30	4.73e-10
ITGAX	integrin subunit alpha X	1.19	4.13e-09
ITGAM	integrin subunit alpha M	1.08	2.23e-09
PLEK	pleckstrin	1.20	1.01e-09

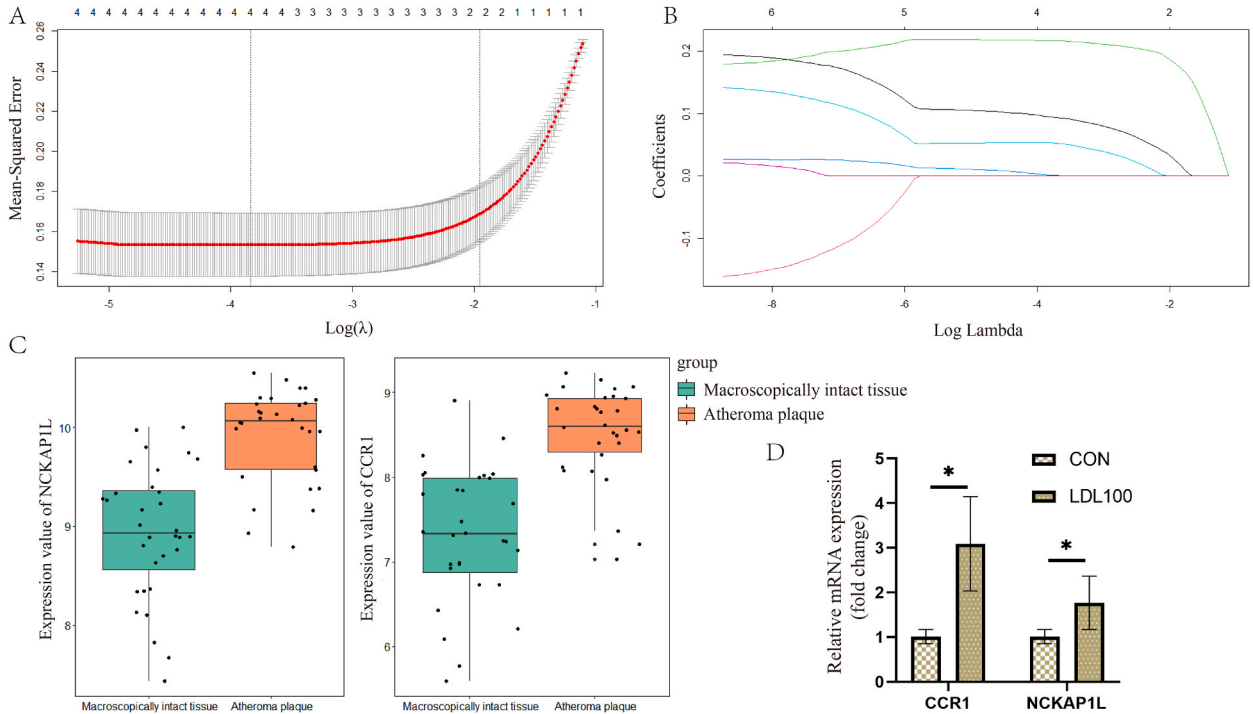


**Fig. 6.** Identification of CCR1 and NCKAP1L. (A) LASSO coefficient profiles of 500 genes. (B) Two genes were taken for selecting  $\lambda$  based on 1-SE criteria for recurrence. (C) Box plot of the two hub genes expression values. (D) The expression levels of the two hub genes in ox-LDL-induced HUVECs. An asterisk (\*) denotes  $P < 0.05$  by independent-sample *t*-test ( $n = 3$ ).

of CCR1 and NCKAP1L in GSE43292. CCR1 and NCKAP1L expression levels were higher in the atheroma plaques than in the macroscopically intact tissues from the patients with hypertension (Fig. 6C). We measured the migration of HUVECs. The migration of HUVECs in the ox-LDL group was 1.58-fold higher than that in the control group. These data indicated that ox-LDL was capable of promoting endothelial cell migration (Fig. 6D and E). We also assessed the mRNA expression of CCR1 and NCKAP1L in ox-LDL-induced HUVECs through an qRT-PCR experiment. As shown in Fig. 6F, the expression of CCR1 and NCKAP1L mRNA was substantially increased compared with the control group. The results of the *in vitro* cell experiments were consistent with the above results.

**4. Discussion**

Atherosclerosis is an autoimmune, dysfunctional inflammatory disease of the vessel wall [20,21]. Endothelial dysfunction is believed to play a crucial role in the pathogenesis of atherosclerosis. Activated endothelial cells secrete chemokines and inflammatory mediators, leading to the recruitment of monocytes and various types of T lymphocytes. This establishes a complex immuno-regulatory network within the atherosclerotic lesion, contributing to lesion progression. Despite significant advancements in the clinical treatment of atherosclerosis, elucidating the precise pathogenesis of atherosclerosis remains a critical challenge. Therefore, it is imperative to understand the underlying molecular mechanisms of endothelial dysfunction.

In the present study, we identified 161 DEGs, with 82 genes showing upregulation and 79 genes showing downregulation in the sample of CAS in patients with hypertension. Subsequently, we developed a WGCNA for atheroma plaques compared with macroscopically intact tissues. The analysis revealed the presence of 11 distinct gene modules within the coexpression network. Among the 11 modules, the gray60 module was most significantly associated with CAS in patients with hypertension. The genes in the gray60

module were subjected to GO and KEGG pathway enrichment analysis. The MM and GS values were set to screen the genes that were most closely related to CAS in the patients with hypertension in the gray60 module. Following this, a set of 249 genes was employed to construct a PPI network through Cytoscape. Subsequently, 11 genes exhibiting the highest interconnected cluster scores, as determined by MCODE, were intersected with the DEGs to identify six hub genes (NCKAP1L, ITGB2, CCR1, ITGAX, ITGAM, PLEK). Among these, the pivotal biomarker CCR1 was ultimately selected through the LASSO algorithm and verified using qRT-PCR.

Pathways related to immune response were clustered in the gray60 module. In recent decades, there has been significant research on the immune mechanisms of atherosclerosis. The research has emphasized the strong correlation between the innate immune system and atherosclerosis, along with plaque instability [22]. Ahrathy et al. [23] demonstrated that treating ApoE<sup>-/-</sup> mice with NK-cell depletion significantly reduced atherosclerosis progression.

CCR1, known as C-C motif chemokine receptor-one, belongs to the beta chemokine receptor family. Signal transduction through CCR1 and its ligand CCL5 plays a crucial role in recruiting effector immune cells, particularly monocytes, to atherosclerosis plaques. Alma et al. [24] demonstrated that in the APOE<sup>-/-</sup> mouse model with left carotid artery injury, deficiency in CCR1 heightened proinflammatory interferon-gamma levels in the neointima, indicating a decrease in macrophage recruitment. Another study revealed that activation of the CCL5/CCR1 axis significantly increased macrophage infiltration in the atherosclerotic vascular wall, thereby exacerbating plaque burden [25]. Moreover, CCR1 is involved in recruiting neutrophils to early atherosclerotic lesions in major arteries [26]. Conversely, some studies have noted that the absence of CCR1 in the APOE<sup>-/-</sup> mouse model promotes aortic root atherosclerosis development and worsens the local accumulation of Th1 cells and IFN-gamma expression [27].

NCKAP1L encodes NCK-associated protein 1 one-like, part of the HEM family of tissue-specific transmembrane proteins. Carla et al. [28] demonstrated that the absence of NCKAP1L resulted in the reversal of the CD4/CD8 ratio in two patients with immune deficiency. Other studies have indicated that NCKAP1L deficiency leads to the inactivation of the Akt/mTOR signaling pathway in human patients with immunodeficiency and immune overactivation [29]. Therefore, NCKAP1L was associated with immune disorders and may play a role in the pathological progression of atherosclerosis.

Pathways related to immune response, such as the immune response-regulating signaling pathway, were clustered in the gray60 module. A previous study has shown a close association of the immune system (involving natural killer cells, macrophages, and DCs) with atherosclerosis, as well as with plaque instability [22]. Ahrathy et al. [23] demonstrated that perforin and granzyme B produced by NK cells promoted lesion growth in atherosclerotic mice, and the depletion of NK cells greatly attenuated atherosclerosis of ApoE<sup>-/-</sup> mice. Marit et al. [30] suggested that dendritic cells with dysregulation of lipid uptake and efflux pathways can modulate inflammatory cytokine secretion and atherogenesis through enhancing T-cell activation and Th1- and Th17-cell polarization. Plaque macrophages predominantly originate from circulating monocytes and display both proinflammatory and anti-inflammatory phenotypes that do not conform strictly to the traditional M1 or M2 classification schemes [31]. Single-cell sequencing has revealed at least five different macrophage subpopulations through identification of biomarkers, which are the main population involved in the formation of atherosclerosis [32,33]. Our enrichment analysis results indicated that the immune-related gene set and signaling pathways were upregulated, which is consistent with recent studies.

Both our study and the study by Sheng et al. [34] utilized the dataset GSE43292 to identify DEGs, build a PPI network, and employ the MCODE algorithm to identify hub genes. However, WGCNA and LASSO were used to further assist in pinpointing the central genes in our study. An endothelial dysfunction cell model was also established using ox-LDL intervention on HUVECs, based on a report from another established model [35]. Furthermore, gene validation was performed through qRT-PCR.

Our study had certain limitations. The lack of detailed clinical information such as the Stary classification in the GEO dataset hindered the association of hub genes with clinical features, potentially compromising the precision of our evaluation of key biomarkers. Carotid plaques are complex structures, and include endothelial cells, fibroblasts, and inflammatory cells [36]. Although we utilized an endothelial dysfunction cell model to pinpoint these hub genes, our reliance on a single cell type for experimental validation may not provide a comprehensive explanation for the biological insights derived from CAS tissue samples in the GSE43292 dataset. Further cellular functional experiments focused on atherosclerotic endothelial dysfunction, incorporating knockdown or over-expression studies, should be employed to elucidate the roles of CCR1 and NCKAP1L more thoroughly. Furthermore, the functions of these genes may not be limited to endothelial dysfunction; they could also be related to changes in smooth muscle cells. Nonetheless, given the pivotal role of endothelial dysfunction in the early stages of atherosclerosis, the identification of genes at the cellular level holds significant reference value for understanding the pathological mechanisms underlying endothelial dysfunction.

## 5. Conclusion

In this study, we used the WGCNA method and LASSO algorithm to identify the key modules and hub genes of CAS in patients with hypertension, and identified two hub genes in the atherosclerotic endothelial dysfunction cell model, providing guidance for the molecular mechanism of CAS plaque lesions. Our study did not directly demonstrate the correlation between the findings of the bioinformatics analysis on CAS in patients with hypertension and endothelial dysfunction; thus, further research is needed to elucidate the intricate molecular mechanisms and biological functions of CAS.

## Data availability statement

All the data for our study were sourced from the publicly available GEO database, and the processing methods along with the resulting data were detailed in the manuscript materials section and figures.

## CRediT authorship contribution statement

**Yimin Wang:** Writing – original draft, Methodology, Conceptualization. **Xinyang Shou:** Writing – original draft, Data curation. **Yuteng Wu:** Visualization, Software, Investigation. **Jun Chen:** Validation. **Rui Zeng:** Supervision. **Qiang Liu:** Writing – review & editing.

## Declaration of competing interest

The authors declare that they have no known competing financial interests or personal relationships that could have appeared to influence the work reported in this paper.

## Acknowledgments

We thank LetPub ([www.letpub.com](http://www.letpub.com)) for its linguistic assistance during the preparation of this manuscript.

## References

- [1] S.C. Bir, R.E. Kelley, Carotid atherosclerotic disease: a systematic review of pathogenesis and management, *Brain Circulation* 8 (3) (2022) 127–136.
- [2] P. Song, et al., Global and regional prevalence, burden, and risk factors for carotid atherosclerosis: a systematic review, meta-analysis, and modelling study, *Lancet Global Health* 8 (5) (2020) e721–e729.
- [3] M. Jusufovic, et al., Blood pressure lowering treatment in patients with carotid artery stenosis, *Curr. Hypertens. Rev.* 12 (2) (2016) 148–155.
- [4] G. Gallo, M. Volpe, C. Savoia, Endothelial dysfunction in hypertension: current concepts and clinical implications, *Front. Med.* 8 (2021) 798958.
- [5] A. Shaito, et al., Oxidative stress-induced endothelial dysfunction in cardiovascular diseases, *Frontiers In Bioscience (Landmark Edition)* 27 (3) (2022) 105.
- [6] M.G. Ziegler, Atherosclerosis and blood pressure variability, *Hypertension* 71 (3) (2018) 403–405.
- [7] M.A. Gimbrone, G. García-Cardeña, Endothelial cell dysfunction and the pathobiology of atherosclerosis, *Circ. Res.* 118 (4) (2016) 620–636.
- [8] P. Libby, et al., Reassessing the mechanisms of acute coronary syndromes, *Circ. Res.* 124 (1) (2019) 150–160.
- [9] T. Quillard, et al., TLR2 and neutrophils potentiate endothelial stress, apoptosis and detachment: implications for superficial erosion, *Eur. Heart J.* 36 (22) (2015) 1394–1404.
- [10] C.A. Sobsey, et al., Targeted and untargeted proteomics approaches in biomarker development, *Proteomics* 20 (9) (2020) e1900029.
- [11] L. Gautier, et al., affy-analysis of Affymetrix GeneChip data at the probe level, *Bioinformatics* 20 (3) (2004) 307–315.
- [12] M.E. Ritchie, et al., Limma powers differential expression analyses for RNA-sequencing and microarray studies, *Nucleic Acids Res.* 43 (7) (2015) e47.
- [13] P. Langfelder, S. Horvath, WGCNA: an R package for weighted correlation network analysis, *BMC Bioinf.* 9 (2008) 559.
- [14] T. Wu, et al., clusterProfiler 4.0: a universal enrichment tool for interpreting omics data, *Innovation* 2 (3) (2021) 100141.
- [15] D. Szklarczyk, et al., STRING v11: protein-protein association networks with increased coverage, supporting functional discovery in genome-wide experimental datasets, *Nucleic Acids Res.* 47 (D1) (2019) D607–D613.
- [16] P. Shannon, et al., Cytoscape: a software environment for integrated models of biomolecular interaction networks, *Genome Res.* 13 (11) (2003) 2498–2504.
- [17] G.D. Bader, C.W.V. Hogue, An automated method for finding molecular complexes in large protein interaction networks, *BMC Bioinf.* 4 (2003) 2.
- [18] S. Engebretsen, J. Bohlin, Statistical predictions with glmnet, *Clin. Epigenet.* 11 (1) (2019) 123.
- [19] X. Shou, et al., miR-126 promotes M1 to M2 macrophage phenotype switching via VEGFA and KLF4, *PeerJ* 11 (2023) e15180.
- [20] D. Wolf, K. Ley, Immunity and inflammation in atherosclerosis, *Circ. Res.* 124 (2) (2019) 315–327.
- [21] K. Kobiyama, K. Ley, Atherosclerosis, *Circ. Res.* 123 (10) (2018) 1118–1120.
- [22] P. Raggi, et al., Role of inflammation in the pathogenesis of atherosclerosis and therapeutic interventions, *Atherosclerosis* 276 (2018).
- [23] A. Selathurai, et al., Natural killer (NK) cells augment atherosclerosis by cytotoxic-dependent mechanisms, *Cardiovasc. Res.* 102 (1) (2014) 128–137.
- [24] A. Zernecke, et al., Deficiency in CCR5 but not CCR1 protects against neointima formation in atherosclerosis-prone mice: involvement of IL-10, *Blood* 107 (11) (2006) 4240–4243.
- [25] J. Jehle, et al., Elevated levels of 2-arachidonoylglycerol promote atherogenesis in ApoE<sup>-/-</sup> mice, *PLoS One* 13 (5) (2018) e0197751.
- [26] M. Drechsler, et al., Hyperlipidemia-triggered neutrophilia promotes early atherosclerosis, *Circulation* 122 (18) (2010) 1837–1845.
- [27] V. Braunersreuther, et al., Ccr5 but not Ccr1 deficiency reduces development of diet-induced atherosclerosis in mice, *Arterioscler. Thromb. Vasc. Biol.* 27 (2) (2007) 373–379.
- [28] C.N. Castro, et al., NCKAP1L defects lead to a novel syndrome combining immunodeficiency, lymphoproliferation, and hyperinflammation, *J. Exp. Med.* 217 (12) (2020).
- [29] S.A. Cook, et al., HEM1 deficiency disrupts mTORC2 and F-actin control in inherited immunodysregulatory disease, *Science (New York, N.Y.)* 369 (6500) (2020) 202–207.
- [30] M. Westerterp, et al., Cholesterol accumulation in dendritic cells links the inflammasome to acquired immunity, *Cell Metabol.* 25 (6) (2017).
- [31] P. Roy, M. Orecchioni, K. Ley, How the immune system shapes atherosclerosis: roles of innate and adaptive immunity, *Nat. Rev. Immunol.* 22 (4) (2022) 251–265.
- [32] A. Zernecke, et al., Meta-analysis of leukocyte diversity in atherosclerotic mouse aortas, *Circ. Res.* 127 (3) (2020) 402–426.
- [33] C. Cochain, et al., Single-cell RNA-seq reveals the transcriptional landscape and heterogeneity of aortic macrophages in murine atherosclerosis, *Circ. Res.* 122 (12) (2018) 1661–1674.
- [34] S. Yan, et al., Identification of ITGAX and CCR1 as potential biomarkers of atherosclerosis via gene set enrichment analysis, *J. Int. Med. Res.* 50 (3) (2022) 3000605211039480.
- [35] V. Lubrano, S. Balzan, LOX-1 and ROS, inseparable factors in the process of endothelial damage, *Free Radic. Res.* 48 (8) (2014) 841–848.
- [36] L.A.V. Baroncini, et al., Histological composition and progression of carotid plaque, *Thromb. J.* 5 (2007) 4.